Adsorption Configuration and Local Ordering of Silicotungstate Anions on Ag(100) Electrode Surfaces

Lien Lee,[‡,†] Jia X. Wang,*[,||] Radoslav R. Adžić,[||] Ian K. Robinson,*[,†,§] and Andrew A. Gewirth*[,†,‡]

Contribution from the Department of Chemistry, Department of Physics, and Frederick Seitz Materials Research Laboratory, University of Illinois at Urbana-Champaign, Urbana, Illinois 61801, and Materials and Chemical Science Division, Department of Applied Science, Brookhaven National Laboratory, Upton, New York 11973

Received May 3, 2001. Revised Manuscript Received July 2, 2001

Abstract: X-ray reflectivity, cyclic voltammetry, and scanning tunneling microscopy (STM) are used to examine the structure of α-$SiW_{12}O_4^{4-}$ or silicotungstic acid (STA) adsorbed on Ag(100) in acid solution. The voltammetry shows that STA passivates the Ag surface relative to electron transfer to a solution redox species. STM images reveal the formation of a series of lattice structures, one of which can be associated with a commensurate $(\sqrt{13}\times\sqrt{13})R33.69°$ structural model. X-ray reflectivity measurements show uniquely that STA orients with its four-fold axis perpendicular to the Ag(100) surface and that the center of the STA molecule is 4.90 Å above the top layer of the Ag substrate. Analysis of bond lengths leads to a footprint of STA on Ag(100), in which the four terminal O atoms are located near the hollow sites and have a Ag−O bond length of 2.06 Å. This bond length is consistent with a strong covalent interaction between STA and the Ag surface.

I. Introduction

We report the results of X-ray reflectivity and scanning tunneling microscopy (STM) measurements examining the structure of an inorganic molecule—α-$H_4SiW_{12}O_{40}$ or silicotungstic acid (STA)—adsorbed on Ag(100) in acid solution. The assembly of molecules onto surfaces from solution is of considerable importance because of the utility of these molecules in modifying electrode behavior by incorporating molecular functionality to the surface.[1−3] Spontaneous adsorption of organic molecules exhibiting these properties onto metal and semiconductor surfaces is well documented. Of particular interest in this work is the strength of the interaction between the surface and the adsorbing molecule. Establishing the degree of interaction between the thiols and Au or Ag surfaces has long been a focus of directed research.[4] However, the thiols are unstable in aggressive environments and are relatively easily reduced or oxidized.[5] Characterization of additional molecular scaffolds as they adsorb onto metal surfaces is thus particularly important.

We showed previously that STA spontaneously forms adherent, ordered monolayer arrays on Ag(111) surfaces when the surface is exposed to the molecule in acidic solution.[6−8] STM images of the adsorbed STA monolayers on Ag(111) or Au(111) revealed a four-fold symmetric structure, and on this basis we proposed that the T_d-symmetric STA molecule was arranged with its S_4 axis perpendicular to the Ag(111) surface.[6,7] This orientation would maximize the number of Ag−O contacts at four and thus be more favored thermodynamically than a structure with the molecular C_3 axis perpendicular to the surface where there would be only three Ag−O contacts. The STA molecule is interesting not only because of its ability to associate with Ag but also because it, and other polyoxometalates, act as partial hydration and oxidation catalysts.[9] Polyoxometalates also have utility in schemes ranging from corrosion protection to biology.[10,11]

One question engendered by this result has to do with the strength of the interaction between the STA molecule and the surface. In studies on more inert materials, such as gold or graphite, the molecule behaves like an anion which is weakly adsorbed on the surface.[12−18] However, the oxophilicity of silver

* To whom correspondence should be addressed.
‡ Department of Chemistry.
§ Department of Physics.
† Frederick Seitz Materials Research Laboratory.
|| Brookhaven National Laboratory.

(1) Dubois, L. H.; Nuzzo, R. G. *Annu. Rev. Phys. Chem.* **1992**, *43*, 437.
(2) Ulman, A. *Ultrathin Organic Films*; Academic Press: San Diego, 1991.
(3) Tredgold, R. H. *Order in Thin Organic Films*; Cambridge University Press: Cambridge, 1994.
(4) Fenter, P.; Schreiber, F.; Berman, L.; Scoles, G.; Eisenberger, P.; Bedzyk, M. J. *Surf. Sci.* **1998**, *413*, 213−235.
(5) Zhang, Y. M.; Terrill, R. H.; Tanzer, T. A.; Bohn, P. W. *J. Am. Chem. Soc.* **1998**, *120*, 2654−2655.
(6) Ge, M. H.; Zhong, B. X.; Klemperer, W. G.; Gewirth, A. A. *J. Am. Chem. Soc.* **1996**, *118*, 5812−5813.
(7) Ge, M. H.; Gewirth, A. A.; Klemperer, W. G.; Wall, C. G. *Pure & Appl. Chem.* **1997**, *69*, 2175−2178.
(8) Klemperer, W. G.; Wall, C. G. *Chem. Rev.* **1998**, *98*, 297−306.
(9) Misono, M.; Okuhara, T. *CHEMTECH* **1993**, *23*, 23−29.
(10) Pope, M. T. *Heteropoly and Isopoly Oxometalates*; Springer-Verlag: Berlin, 1983.
(11) Pope, M. T., Muller, A., Eds. *Polyoxometalates: From Platonic Solids to Anti-Retroviral Activity*; Kluwer Academic Publishers: Dordrecht, 1994; Vol. 10.
(12) Watson, B. A.; Barteau, M. A.; Haggerty, L.; Lenhoff, A. M. *Langmuir* **1992**, *8*, 1145−1148.
(13) Keita, B.; Nadjo, L. *J. Electroanal. Chem.* **1993**, *354*, 295−304.
(14) Keita, B.; Nadjo, L. *Surf. Sci. Lett.* **1991**, *254*, L443−L447.
(15) Dong, S.; Baoxing, W. *Electrochim. Acta* **1992**, *37*, 11−16.
(16) Ge, M.; Niece, B. K.; Wall, C. G.; Klemperer, W. G.; Gewirth, A. A. In *Electrochemical Synthesis and Modification of Materials*; Andricacos, P. C., Corcoran, S. G., Delplancke, J.-L., Moffat, T. P., Searson, P. C., Eds.; 1997; Vol. 451, pp 99−108.
(17) Liu, S.; Tang, Z.; Shi, Z.; Niu, L.; Wang, E.; Dong, S. *Langmuir* **1999**, *15*, 7268−7275.
(18) Cheng, L.; Dong, S. J. *J. Electrochem. Soc.* **2000**, *147*, 606−612.

10.1021/ja0161352 CCC: $20.00
Published on Web 08/10/2001

gives rise to the possibility that the STA molecule could be covalently attached through terminal oxo groups presented to the Ag surface. This covalent attachment could in concept provide unique opportunities for surface modification. We report here the results of in situ STM and X-ray reflectivity measurements which provide information on the local ordering and the adsorption configuration of STA molecules on Ag(100). The bond lengths calculated from the interface structures determined in this study uniquely establish that STA interacts strongly with the Ag surface.

II. Experimental Section

All solutions were prepared in purified water (Milli-Q UV plus, 18.2 M Ω cm). The supporting electrolyte was $HClO_4$ (J.T. Baker, ULTREX II Ultrapure Reagent). α-$H_4SiW_{12}O_4$ was prepared following published procedures[19] and recrystallized from purified water. The typical α-$SiW_{12}O_4^{4-}$ concentration was 5×10^{-4} M. Freshly flame-annealed Au or Pt wires were used as the counter electrode. A AuO wire was used as the reference electrode for STM measurements, a Ag/AgCl reference was used for the voltammetry, and a reversible hydrogen electrode[20] in 0.1 M $HClO_4$ was used in X-ray measurements. All potentials are reported relative to normal hydrogen electrode (NHE). Voltammetry was obtained using a potentiostat and a two-compartment cell that was purged prior to use.

STM images were obtained with a NanoScope III E electrochemical STM (ECSTM) equipped with a fluid cell (Digital Instruments) or a Molecular Imaging STM. The tip was formed from a Pt/Ir wire coated with polyethylene except at the very tip to minimize the Faradaic background. Substrates were formed from a Ag(100) single crystal (Monocrystals) prepared according to published procedures.[21,22] Atomic resolution in situ STM images revealed the expected (100) texture with at least 50 nm wide terraces.

X-ray specular reflectivity measurements were carried out at the National Synchrotron Light Source (NSLS) at beam line X22A using monochromatic X-rays with $\lambda = 1.20$ Å. The Ag(100) single crystal was oriented within 0.2 degrees of the (100) crystallographic plane. After chemical polishing using CrO_3/HCl solution,[21,22] the sample was cleaned in H_2SO_4 and H_2O and transferred into an electrochemical X-ray scattering cell with a drop of water covering the surface. A body-centered tetragonal coordinate system was used to describe the reciprocal space vector, $Q = |H\vec{a}^* + K\vec{b}^* + L\vec{c}^*|$, where $a^* = b^* = 2\pi/a$, $c^* = 2\pi/\sqrt{2}a$. For Ag(100), $a = 2.889$ Å, and L is along the surface normal direction. All of the integrated intensities were measured with a 2 mm × 2 mm slit located 600 mm from the sample. The resulting resolution in the surface plane is larger than the intrinsic peak width for all measured reflections.

III. Results and Discussion

3.1. Voltammetric Measurements. The dashed line in Figure 1 shows a cyclic voltammogram from a Ag(100) electrode immersed in a solution containing 0.5 mM $H_4SiW_{12}O_{40}$ + 0.1 M $HClO_4$. The voltammogram is essentially featureless except for a small amount (ca. 10 μA/cm^2) of capacity current in the potential range from +0.5 to −0.2 V. The cathodic current evident at more negative potentials results either from reduction of residual oxygen present in the cell or from nascent hydrogen evolution. The lack of features is surprising because the first reduction peak of α-$SiW_{12}O_{40}^{4-}$ occurs at 0.0 V on other working electrodes.[23] For example, in measurements performed with a Au(111) electrode (Figure 1, solid line), the first STA redox peak is observed at 0.0 V which corresponds to a one-electron redox reaction of solution STA species.[23] The lack of any current at this potential on Ag(100) indicates that the surface is passivated so that no discernible electron transfer between the surface and solution STA occurs. We note as well that there is no apparent contribution to the voltammetry from STA already adsorbed on the Ag(100) electrode surface. The lack of features here suggests that STA adsorbed on the surface might be stabilized relative to solution STA and exhibit a first redox peak at potentials outside (negative) of the region interrogated in this voltammogram.

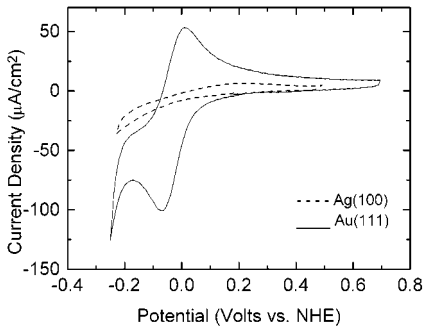

Figure 1. Cyclic voltammograms obtained from solutions containing 0.5 mM STA + 0.1 M $HClO_4$ on Ag(111) (dashed line) and Au(111) (solid line) electrode surfaces. Scan rate was 25 mV/s.

3.2. STM Measurements. Figure 2A shows an STM image of a partial monolayer of α-$SiW_{12}O_{40}^{4-}$ adsorbed on a Ag(100) single crystal in 0.5 mM α-$SiW_{12}O_{40}^{4-}$ + 0.1 M $HClO_4$ solution under open circuit potential conditions (ca. 0.45 V). The anions form small domains on the Ag(100) surface with a high number of unoccupied sites. There is no obvious dominant periodicity in the small domains, but in selected areas a certain degree of order can be seen. In particular, the image shows vestiges of rows and squares. The distances between the bright spots range between 1.1 and 1.5 nm. These spacings are consistent with those expected for STA arrays, and the features are thus assigned to STA adsorbed on the Ag(100) surface.

Somewhat more laterally ordered monolayers of STA could be formed by applying a potential more negative than the open circuit potential to the Ag(100) electrode. Figure 2B shows an STM image obtained from a solution containing 0.1 M $HClO_4$ + 0.5 mM α-$SiW_{12}O_{40}^{4-}$ following application of a potential of 0.25 V. Many domains with size ranging from 10 to 20 nm across are seen. There are several locally ordered structures seen in the STM image. Among them, rhombic as well as square patterns were seen with spacings ranging from 0.97 to 1.43 nm. In multiple measurements, fewer apparently empty sites and more ordered domains were observed following poising the surface at negative potentials relative to surfaces maintained at open circuit. This suggests that STA has more opportunity to anneal on the Ag(100) surface under these conditions than at open circuit potential. Because the diffusion length is related to the one-sixth power of ratio of the diffusion constant to the flux,[24] more ordered arrays may arise as a consequence[25] of the decreased flux of STA to the surface at the more negative potentials while the diffusivity of the molecule on the surface remains approximately constant. This behavior is found for Ag adatoms by themselves.[26]

(19) Teze, A.; Herve, G. *Inorg. Synth.* **1990**, *27*, 71−135.
(20) Bard, A. J.; Faulkner, L. R. *Electrochemical Methods*; John Wiley and Sons: New York, 1980.
(21) Hamelin, A.; Stoicoviciu, L.; Doubova, L.; Trasatti, S. *J. Electroanal. Chem.* **1988**, *244*, 133.
(22) Kurasawa, T. Japanese Patent 35005619, 1960.
(23) Herve, G. *Ann. Chim.* **1971**, *6*, 219−228.
(24) Pimpinelli, A.; Villain, J. *Physics of Crystal Growth*; Cambridge University Press: New York, 1998.
(25) Doudevski, I.; Hayes, W. A.; Schwartz, D. K. *Phys. Rev. Lett.* **1998**, *81*, 4927−4930.
(26) Giessen, M.; Dietterle, M.; Stapel, D.; Ibach, H.; Kolb, D. M. *Surf. Sci.* **1997**, *384*, 168.

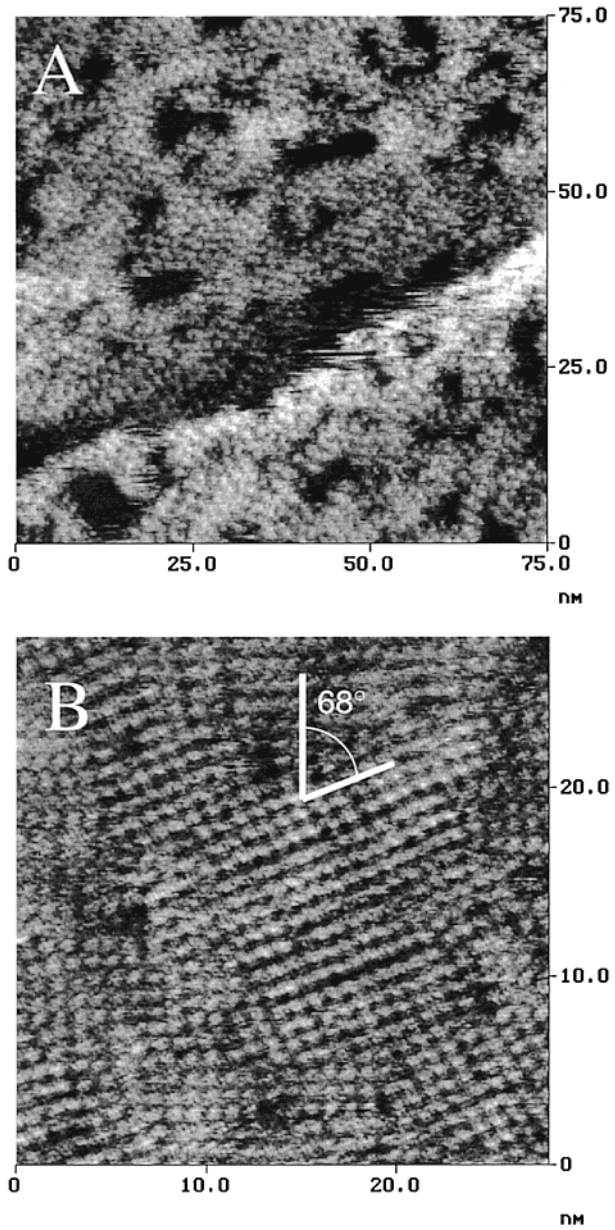

Figure 2. In situ STM images of STA adsorbed on Ag(111) surfaces obtained from solutions containing 0.5 mM STA + 0.1 M $HClO_4$. (A) 75 nm × 75 nm image obtained at open circuit potential. E_{bias}= 294 mV, I_{tip} = 1.69 nA. The angle between two of the domains is shown. (B) 30 nm × 30 nm image obtained following application of a potential of 0.25 V vs NHE. E_{bias}= 143 mV, I_{tip}= 4.20 nA.

One common motif in these domains is a structure with dimensions of 0.98 ± 0.06 nm × 1.00 ± 0.06 nm with an angle between these vectors of 93 ± 5°. These unit cell parameters match $\sqrt{13}$ times the Ag−Ag distance (1.042 nm) on Ag(100) surface. By comparing the orientation of the square STA superlattice with the observed Ag(100) lattice directions, we obtain an angle of 34 ± 5° between the Ag and STA lattices. These parameters are consistent with a commensurate $(\sqrt{13}\times\sqrt{13})R33.69°$ structural model as shown in Figure 3.

The image in Figure 2 evinces several domains exhibiting the lattice parameters detailed above. The angle made between two of these domains, marked in Figure 2, is 68°, which is twice the rotation angle made with the underlying Ag(100) lattice. The observation of this rotation angle is further support for the model shown in Figure 3.

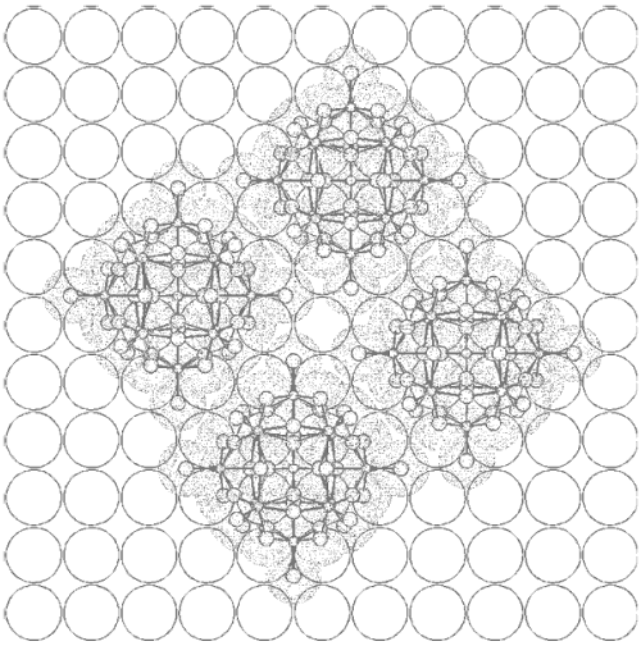

Figure 3. Model of the ($\sqrt{13}$ × $\sqrt{13}$) overlayer of STA on Ag(100) deduced from the STM images. van der Waals radii for the STA molecule are included.

In this model, the STA molecules are adsorbed with the S_4 symmetry axis perpendicular to the surface, which is considered favorable because it allows maximum Ag−O contacts and four-fold symmetry match with the substrate. In this tightly packed lattice, only certain in-plane orientations are possible without terminal oxygens of two adjacent STA molecules closing to within less than the sum of their van der Waals radii ($d_{O\cdots O}$ = 0.28 nm). The orientation with the outmost oxygen atoms oriented collinear with the Ag(100) substrate axes is shown in Figure 3. This configuration, with the STA molecules centered in the hollow sites, allows all four lowest O atoms to be near four-fold hollow sites on the substrate that could enhance the stability of the structure.

3.3. X-ray Specular Reflectivity Measurements. To evaluate these and other features of the STA−Ag interaction, we performed X-ray specular reflectivity measurements on this interface. X-ray specular reflectivity refers to the scattering intensity profile measured along surface normal direction, L, with zero in-plane component ($H = K = 0$). Figure 4 shows the measured specular reflectivity from Ag(100) at 0.1 V in 0.1 M $HClO_4$ solution containing 0.5 mM STA, which was normalized to have the intensities near the Bragg positions (i.e, with L close to 2 and 4) close to the calculated values using eq 1. Far from the Bragg peaks, intensities are sensitive to the surface structure. On the bare Ag(100) surface, the specular reflectivity appears as a featureless curve shown as the dotted line in Figure 4. However, the addition of STA to the Ag(100) surface gives rise to oscillatory behavior most evident below L = 2 which is plotted as open circles in Figure 4. This feature was repeatedly observed in the solutions containing 0.1 to 10 mM STA in the potential region we studied. We found that the data with L less than 0.5 (obtained at very low angles) have large uncertainties due to their sensitivity to instrument setup and hence are excluded in analysis.

In the kinematic approximation, the reflectivity $R(0,0,L)$ is related to the sum over atomic layers with the appropriate atomic form and phase factors for each layer.[27,28] For an ideally

(27) Robinson, I. K.; Tweer, D. J. *Rep. Prog. Phys.* **1992**, *55*, 599.

terminated Ag(100) surface, the reflectivity at large L where the enhancement near the critical angle can be ignored is given by

$$R_{Ag}(0,0,L) = (2r_0/cL)^2 \left| f_{Ag}(L)\, e^{-W(L)} \sum_{n=0}^{-\infty} e^{i\pi nL} \right|^2 \qquad (1)$$

where r_0 is the classical radius of the electron, c (=4.086 Å) is the Ag(100) lattice spacing, $f_{Ag}(L)$ is the atomic form factor, and $W(L) = (2\pi L\sigma/c)^2/2$ is the Debye−Waller factor in which the root-mean-square (rms) amplitude, σ, is a constant for all the layers.

The oscillatory behavior in Figure 4 is associated mainly with constructive and destructive interference of the X-rays by the planes of *W* atoms from the STA molecule. We employed a model to describe the structural properties of a STA adlayer which involves three adjustable parameters: θ, the molecular coverage with respect to the atomic density of the Ag(100) surface, Z, the overall distance between the central Si atom and the topmost Ag layer, and σ, the rms amplitude for all the Si, O, and W atoms. Coordinates for STA were obtained from a published crystal structure for $(H_5O_2)_3(PW_{12}O_{40})$[29] which is very closely related to that of STA.[30] Assuming the molecule does not change shape upon binding to the surface, all the atoms in the STA molecule can be referenced to the parameter Z. Thus, the scattering factor for a monolayer of STA on Ag(100) is given by

$$F_{STA}(L) = (f_{Si}(L) + f_W(L)\sum_{j=1}^{12} e^{2\pi i L z_{W(j)}/c} + f_O(L)\sum_{j=1}^{40} e^{2\pi i L z_{O(j)}/c}) \qquad (2)$$

where $z_{W(j)}$ and $z_{O(j)}$ are the spacing along the surface normal direction with respect to the Si atom. This expression is dependent on the geometry adopted by the STA molecule but has no adjustable parameters. The final form of the specular reflectivity is given by

$$R(0,0,L) = (2r_0/cL)^2 \left| f_{Ag}(L)\, e^{-W(L)} \sum_{n=0}^{-\infty} e^{i\pi nL} + \theta\, e^{2\pi i LZ} e^{-W(\sigma,L)} F_{STA}(L) \right|^2 \qquad (3)$$

Since the adlayer influence often causes a slight top layer expansion or contraction relative to the bulk spacing and the surface layer of a substrate often exhibits an enhanced rms amplitude in the Debye−Waller factor, we have adjusted the summation over the Ag layers to allow the spacing between the top and the second Ag layers (c_0) and the rms amplitude for the top Ag layer (σ_0) to vary in the fitting. This gives six parameters including the scale factor for each atom.

Values for $z_{W(j)}$ and $z_{O(j)}$, and hence the function $F_{STA}(L)$, depend on whether the S_4 or C_3 symmetry axis is perpendicular to the surface. Both models were tried in the analysis. Note that the heavy W atoms are in three planes with four in each for the S_4 model, and with three in the top and bottom planes and six in the middle plane for the C_3 model as shown in Figure 5. These arrangements result in a large difference in the electron density profile along the surface normal direction, and hence distinctly different X-ray specular reflectivity profiles are expected for the two models. An excellent fit was obtained using the S_4 model (solid line in Figure 4), while the C_3 model failed to reproduce the main features in the data (dashed line).

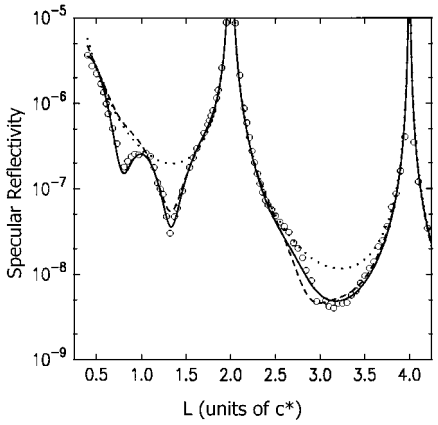

Figure 4. Specular reflectivity (circles) measured for Ag(100) at 0.1 V in 0.1 M $HClO_4$ containing 0.5 mM STA. The dotted line shows the curve for an ideal Ag(100) crystal. The solid and dashed lines are the best fits using the models with the S_4 and C_3 symmetry axis perpendicular to the surface, respectively. Parameters obtained from the best fit to the S_4 model are $\theta = 0.054 \pm 0.004$, $Z = 4.90 \pm 0.02$ Å, and $\sigma = 0.56 \pm 0.03$ Å for the STA adlayer; $Z_0 = 2.027 \pm 0.005$ Å and $\sigma_0 = 0.16 \pm 0.02$ Å for the top Ag layer.

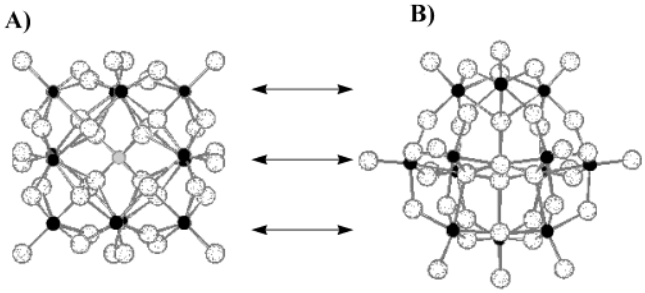

Figure 5. Side views of STA with (A) S_4 and (B) C_3 orientation relative to the Ag(100) surface. W atoms are represented by black circles, O atoms by open circles, and Si by gray circles. The arrows point to the planes of W atoms. There are three planes of W atoms in both cases, but the C_3 model features planes with three, six, and three W atoms while the S_4 case has three planes of four W atoms each.

By far the biggest contribution to the diffraction signal comes from the layers of tungsten atoms in the STA molecular structure. It is therefore possible to model the reflectivity in a more general way by three simple planes of atoms, with adjustable positions. This model is then independent of the assignment of the S_4 or C_3 axis. When we tried this, a fit was obtained that was comparable with the best fit shown in Figure 4. The independently refined layer spacings between the planes of W atoms were 2.40 and 2.55 Å, which agree rather well with the plane separation of 2.51 Å expected for the S_4 orientation, but not with the 2.79 and 3.02 Å expected for the C_3 orientation. Taken together, both modeling procedures indicate that the STA molecules are adsorbed with their S_4 axis perpendicular to the surface.

The Si−Ag layer spacing from the best fit to the S_4 model was $Z = 4.90$ Å (the other parameters are reported in the caption to Figure 4). This value places severe constraints on possible binding sites for STA. We calculated the Ag−O bond lengths for STA molecules on top, bridge, and hollow sites of the Ag(100) lattice with the outmost oxygen atoms collinear with or 45° away from the substrate lattice axes. Only in the

(28) Gibbs, D.; Ocko, B. M.; Zehner, D. M.; Mochrie, S. G. J. *Phys. Rev. B* **1988**, *38*, 7303.
(29) Brown, G. M.; Noe-Spirlet, M.-R.; Busing, W. R.; Levy, H. A. *Acta Crystallogr.* **1977**, *B33*, 1038−1046.
(30) Fuchs, J.; Thiele, A.; Palm, R. *Z. Naturforsch.* **1981**, *86b*, 161−171.

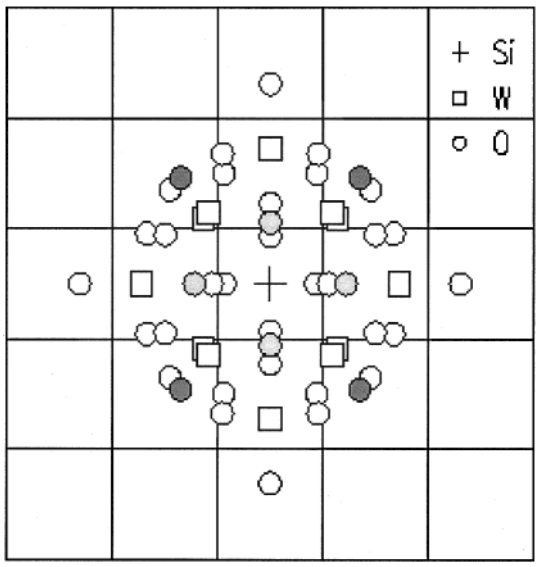

Figure 6. Projection of a STA adsorbate on Ag(100) in the proposed adsorption configuration. The intersection points on the grid represent the position of the Ag atoms. Dark-shaded circles represent the four terminal O atoms which have a Ag−O separation of 2.06 Å. The lighter shaded circles represent the two pairs of bridging O atoms which have Ag−O separations of 2.23 and 2.43 Å.

configuration shown in Figure 6 (centered in the hollow sites with the terminal O atoms aligned with the (10) and (01) substrate lattice axes) are all of the O atoms in positions far from the Ag atoms of the substrate, so that the shortest Ag−O bond length is not smaller than the sum of their covalent radii (2.00 Å).[31] This suggests a unique adsorption site of STA on Ag(100). Not only the molecule's orientation along the surface normal direction but also the in-plane orientation (around that axis) and lateral position are the same for the STA molecules adsorbed on the Ag(100) surface.

The Ag−O bond lengths in this model are 2.06 Å for the four terminal oxygen atoms and 2.23 and 2.43 Å for the two pairs of lowest bridging oxygen atoms in the STA molecule. The Ag−O distance for the terminal oxo groups is consistent with the Ag−O distance (2.05 ± 0.03 Å) found in the (2 × 1)O/Ag(110) missing row reconstructed surface[32,33] where a very strong chemisorption interaction between Ag and O is known to occur.[34] By way of contrast, the Ag−O spacing obtained from surface extended X-ray adsorption fine structure (SEXAFS) measurements for what is either water or perchlorate physisorbed atop an underpotentially deposited monolayer of Ag on Au(111) was either 2.21 Å[35] or 2.42 Å,[36] and the surface carbonate species on Ag(110)—known to have partial ionic character—exhibits a Ag−O bond length of 2.8 Å.[37]

The adsorption configuration deduced from the X-ray reflectivity measurements fits well to the ($\sqrt{13} \times \sqrt{13}$) in-plane lattice observed by STM. In Figure 3 we showed that one possible configuration for STA on Ag(100) deduced from the STM is with the lowest terminal oxo groups near the four-fold hollow sites. The STM alone cannot distinguish between this and other possible footprints for the STA molecule. Our results suggest that the commensurate ($\sqrt{13} \times \sqrt{13}$) phase does not cause much strain with respect to a free-standing STA layer in which the in-plane orientation is determined by minimizing the intermolecular repulsion. The X-ray data strongly indicate that the registered footprint of the molecule with the Ag surface is the correct choice. This argument also supports the uniqueness of the adsorption configuration for STA on Ag(100).

There are other low-coverage lattices exhibiting the same STA footprint on the Ag surface which should also be commensurate with the Ag(100) lattice. There are five commensurate lattice constants, $\sqrt{13}$, 4, $\sqrt{17}$, $\sqrt{18}$, and $\sqrt{20}$ in units of Ag lattice constant ($a = 0.289$ nm), in the range from 0.97 to 1.43. The coverages for a square lattice with these lattice spacings are $1/13 = 0.077$, $1/16 = 0.0625$, $1/17 = 0.059$, $1/18 = 0.056$, and $1/20 = 0.050$, respectively. The STA coverage obtained from the best fit of the specular reflectivity is 0.054. This is closest to the 1/18 coverage obtained for the ($\sqrt{18} \times \sqrt{18}$) square and ($\sqrt{18} \times \sqrt{20}$) rhombic lattices. However, lattices with a range of spacings have been observed by STM, which suggests that the 0.054 coverage results from an average over several locally ordered lattices. A more detailed X-ray diffraction study on the coexisting phases will be reported elsewhere.

IV. Conclusions

Local ordering of the STA monolayer on the Ag(100) electrode surface has been observed in STM images which exhibit lattice spacings ranging from 0.97 to 1.43 nm. One of these, the ($\sqrt{13}\times\sqrt{13}$)*R*33.69° motif, has the highest density, and the adsorption configuration proposed for this lattice is consistent with the results of our X-ray reflectivity study. Distinctly different features are expected in the specular reflectivity for STA molecules oriented with their S_4 or C_3 symmetry axis perpendicular to the surface because the electron density profile along the surface normal direction is very different for the two models. The data clearly suggest an adsorption configuration with the S_4 axis perpendicular to the surface and 4.90 Å spacing between the center of the STA molecule and the Ag surface layer. From this spacing, the Ag−O bond lengths were calculated for different in-plane configurations. The only configuration which does not feature an Ag−O bond length shorter than 2.0 Å is one where the STA molecules are centered in the Ag(100) hollow sites and with outmost terminal O atoms collinear with the substrate lattice axes. This configuration places the four lowest terminal O atoms near four-fold hollow sites on the Ag(100) surface. The Ag−O bond length is 2.06 Å for these four contacting O atoms in this configuration. This distance is within the range of Ag−O bond lengths formed by oxygen on the Ag(110) adlattice in the (2 × 1) missing row structure where a strong covalent bond is known to occur. The congruence of these bond lengths suggests very strongly that formation of a chemisorption bond between the Ag surface and terminal O atoms of the STA molecule has occurred. This covalent interaction between STA and Ag has consequences both in passivating the Ag surface toward electron transfer to a solution redox species and possibly in stabilizing the STA adsorbed on the Ag surface itself.

These results demonstrate that STA can strongly adsorb to Ag much in the same manner by which thiolates can adsorb on Au but with an entirely different chemistry. The strong interaction between Ag and STA—and by extension other polyoxometalates—can now be utilized to tune electrode properties in areas such as catalysis and corrosion protection, and this is work in progress.

(31) Emsley, J. *The Elements*, 2nd ed.; Clarendon Press: Oxford, 1991.
(32) Puschmann, A.; Haase, J. *Surf. Sci.* **1984**, *144*, 559−566.
(33) Becker, L.; Aminpiroz, S.; Schmalz, A.; Hillert, B.; Pedio, M.; Haase, J. *Phys. Rev. B* **1991**, *44*, 13655−13659.
(34) Besenbacher, F.; Nørskov, J. K. *Prog. Surf. Sci.* **1993**, *5*, 5−66.
(35) Samant, M. G.; Borges, G.; Melroy, O. R. *J. Electrochem. Soc.* **1993**, *140*, 421−425.
(36) White, J. H.; Albarelli, M. J.; Abruna, H. D.; Blum, L.; Melroy, O. R.; Samant, M. G.; Borges, G. L.; Gordon, J. G. I. *J. Phys. Chem.* **1988**, *92*, 4432−4436.
(37) Bader, M.; Hillert, B.; Puschmann, A.; Haase, J.; Bradshaw, A. M. *Europhys. Lett.* **1988**, *5*, 443−448.

Acknowledgment. We thank Mr. Jason Powell for providing the STA used in this work and Dr. Ben Ocko and Dr. Walter Klemperer for useful discussions. This work was funded by Department of Energy Grant DE-FG02-91ER45439 through the Materials Research Laboratory at the University of Illinois and by the Department of Energy under Contract DE-AC02-98CH10886 for the X-ray measurements carried out at Brookhaven National Laboratory. A.A.G. acknowledges the NSF (CHE 9820828) for partial support of this research.

JA0161352